Electronic Supplementary Information

for

POSS-containing Red Fluorescent Nanoparticles for Rapid Detection of Aqueous Fluoride Ions

Fanfan Du, Yinyin Bao, Bin Liu, Jiao Tian, Qianbiao Li, and Ruke Bai*

CAS Key Laboratory of Soft Matter Chemistry, Department of Polymer Science and Engineering, University of Science and Technology of China, Hefei, P. R. China 230026.

E-mail: bairk@ustc.edu.cn

Tel: 0086-551-3600722; Fax: 0086-551-3631760

Experimental Section

Aminopropylheptakis (isobutyl) POSS (POSS-NH_2, 97%) was obtained from Hybrid Plastics. 3,4:9,10-Perylenetetracarboxylic dianhydride (98%) was purchased from Sigma-Aldrich. Anionic compounds such as $[Bu_4N]^+Cl^-$, $[Bu_4N]^+Br^-$, $[Bu_4N]^+I^-$, $[Bu_4N]^+HCOO^-$, $NaNO_3$, NaOAc and NaH_2PO_4 were purchased from Shanghai Chemical Co.. $[Bu_4N]^+F^-$ (TBAF, 1 M in THF) was purchased from J&K Chemical Co.. They were used without further purification. Monopotassium salt of 3,4:9,10-perylenetetracarboxylic dianhydride and dodecyl-PAI were synthesized according to literatures (*Dyes and Pigments*, 2006, **69**, 118). All other reagents and solvents were purchased commercially and used without further purification.

POSS-PAI: Monopotassium salt of 3,4:9,10-perylenetetracarboxylic dianhydride (1.0 g, 2.2 mmol) and aminopropylheptakis (isobutyl) POSS (1.92 g, 2.2 mmol) were suspended in water (50 mL). Propanol (50 mL) was added and the mixture was then stirred at 90 °C. Hydrochloric acid was added to stop the reaction after 12 h. The turbid liquid was filtered using a sand core funnel with the aid of a vacuum, and then

washed by methanol. The filter residue was dissolved in chloroform and insoluble substance was subsequently filtered off. The yellow solution was rotary concentrated and further purified on a silica gel column using CH_2Cl_2 as eluent, affording POSS-PAI as red solid (0.63 g, yield: 23%). ^{1}H NMR ($CDCl_3$; 400 MHz): δ = 8.71 (d, J = 8.0 Hz, 2H, ArH), 8.68 (d, J = 8.0 Hz, 2H, ArH), 8.66 (d, J = 8.0 Hz, 2H, ArH), 8.63 (d, J = 8.0 Hz, 2H, ArH), 4.21 (t, J = 7.2 Hz, 2H, NCH_2), 1.91-1.79 (m, 9H, β-CH_2 and CH × 7), 0.97-0.93 (m, 42H, CH_3 × 14), 0.61-0.57 (m, 16H, $SiCH_2$ × 8) (Fig. S2); ^{13}C NMR ($CDCl_3$; 100 MHz): δ = 163.0, 159.9, 136.4, 133.8, 133.6, 131.9, 131.4, 129.4, 126.8, 126.6, 124.1, 123.9, 123.2, 119.08, 43.0, 25.7, 23.9, 22.5, 22.4, 9.8 (Fig. S3). IR (KBr, cm^{-1}): 2956-2873, 1763, 1734, 1694, 1656, 1590, 1505, 1403, 1316, 1229, 1110, 811, 741, and 486. Anal. Calcd for $(C_{55}H_{77}NO_{17}Si_8)$n: C 52.89%; H 6.21%; N 1.12%. Found: C 52.81%; H 6.29%; N 1.11%.

POSS-PBI-PEO: POSS-PAI (0.25 g, 0.2 mmol), methoxypolyethylene glycol amine (0.6 g, 0.3 mmol, M_w = 2 kDa) and dioxane (50 mL) were vigorously stirred under nitrogen at 120 °C for 12 h. After the reaction, the organic solution was rotary concentrated and further purified on a silica gel column using CH_2Cl_2/methanol (V/V = 40/1) as eluent (0.56 g, yield: 87%). ^{1}H NMR ($CDCl_3$; 400 MHz): δ = 8.64 (m, 4H, ArH), 8.59 (m, 4H, ArH), 4.46 (t, J = 6.0 Hz, 2H, PEO-NCH_2), 4.20 (t, J = 7.2 Hz, 2H, POSS-NCH_2), 3.87-3.53 (m, 178H, PEO-CH_2), 3.37 (s, 3H, OCH_3), 1.88-1.79 (m, 9H, β-CH_2 and CH × 7), 0.97-0.93 (m, 42H, CH_3 × 14), 0.61-0.57 (m, 16H, $SiCH_2$ × 8) (Fig. S4); ^{13}C NMR ($CDCl_3$; 100 MHz): δ = 163.5, 163.3, 134.7, 134.5, 131.5, 131.4, 129.5, 129.4, 126.5, 123.5, 123.3, 123.2, 123.1, 72.9, 72.1, 70.7, 70.5, 70.4, 70.2, 68.0, 59.1, 43.0, 39.4, 25.8, 24.0, 22.6, 22.5, 9.9 (Fig. S5).

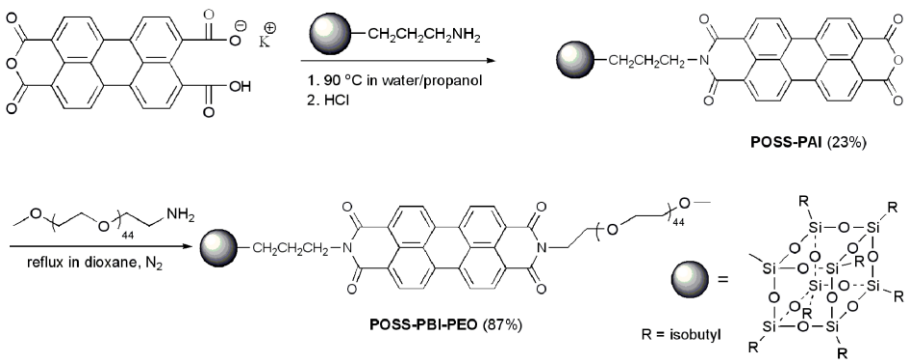

Figure S1. Synthesis procedure of the PBI-bridged amphiphilic polymer POSS-PBI-PEO.

Characterization

Nuclear Magnetic Resonance Spectroscopy (NMR). NMR spectra were recorded on a Bruker AVANCE Ⅱ spectrometer (resonance frequency of 400 MHz for ^{1}H) operated in the Fourier transform mode. $CDCl_3$ and TMS were used as the solvent and internal standard, respectively.

Fourier-transfer infrared Spectroscopy (FT-IR). FT-IR spectra were recorded on a Vector-22 FTIR instrument and were collected at 64 scans with a spectral resolution of 4 cm^{-1}.

Elemental analyses. Elemental analyses were performed on a VARIO ELIII C, H, and N analyzer.

Ultraviolet-Visible Spectroscopy (UV-vis). UV-Vis spectra of solutions were recorded with a Pgeneral UV-Vis TU-1901 spectrometer.

Photoluminescence (PL) Spectroscopy. Emission spectra of solutions were measured by an F-4600 PL Spectrometer. The quantum yield of the NPs in aqueous solution was determined according to the following equation:

$$\Phi_u = \Phi_s \frac{F_u A_s n_u^2}{F_s A_u n_s^2}$$

Where Φ is quantum yield; *F* is integrated area under the corrected emission spectra; *A* is absorbance at the excitation wavelength; *n* is the refractive index of the solution; the subscripts *u* and *s* refer to the unknown and the standard, respectively. Rhodamine B in ethanol (5.0 μg/mL) was used as the standard.

Transmission Electron Microscopy (TEM). TEM observations were conducted on an H-7650 transmission electron microscope at an acceleration voltage of 100 kV. The sample for TEM observations was prepared by placing 10 μL of micellar solution on copper grids.

Dynamic Laser Light Scattering (DLS). A commercial spectrometer (ALV/DLS/SLS-5022F) equipped with a multi-tau digital time correlator (ALV5000) and a cylindrical 22 mW UNIPHASE He-Ne laser (λ_0 = 632 nm) as the light source was employed for DLS measurements. Scattered light was collected at a fixed angle of 90° for duration of 10 min.

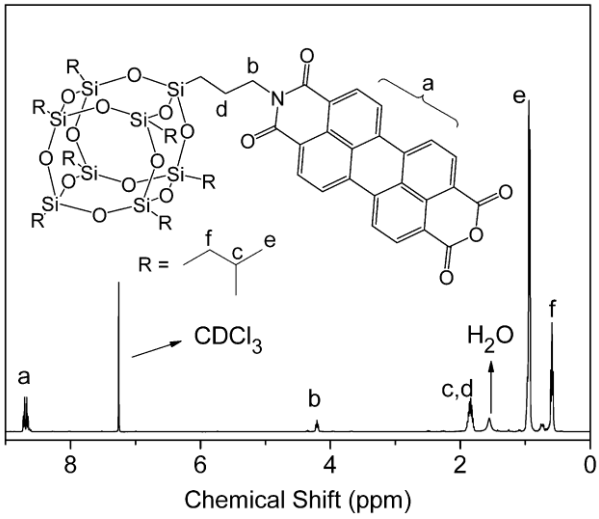

Figure S2. ^{1}H NMR spectrum of POSS-PAI in $CDCl_3$.

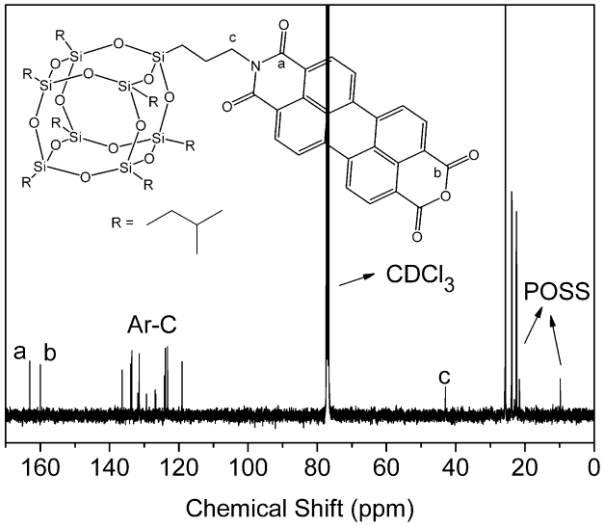

Figure S3. ^{13}C NMR spectrum of POSS-PAI in $CDCl_3$.

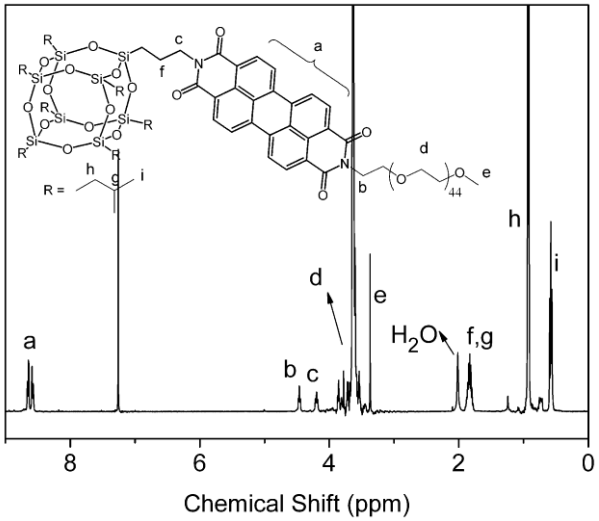

Figure S4. ^{1}H NMR spectrum of POSS-PBI-PEO in $CDCl_3$.

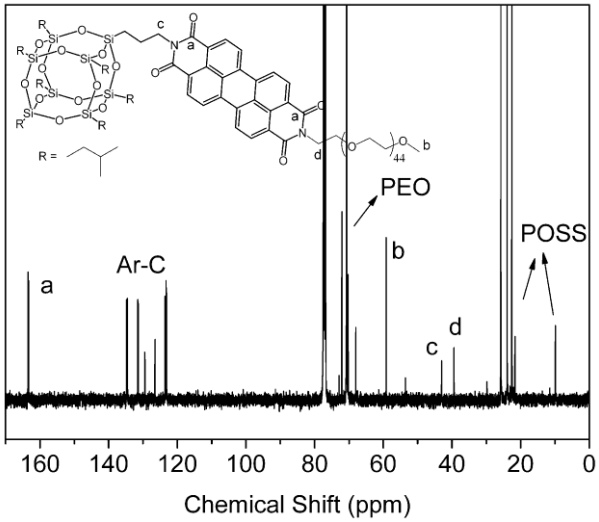

Figure S5. ^{13}C NMR spectrum of POSS-PBI-PEO in $CDCl_3$.

NPs self-assembled from POSS-PBI-PEO in aqueous solution

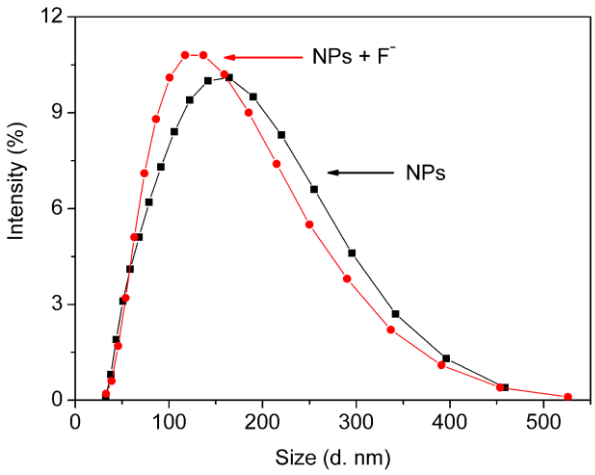

Figure S6. Hydrodynamic radius distributions obtained for hybrid nanoparticles self-assembled from 0.5 g/L aqueous solution of POSS-PBI-PEO before and after the addition of 1 mM TBAF.

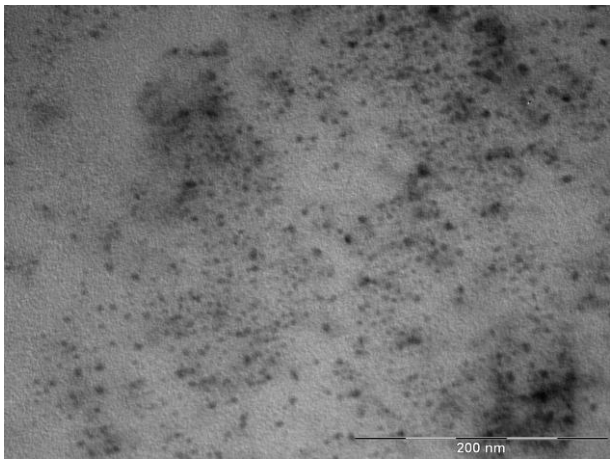

Figure S7. TEM image obtained for hybrid nanoparticles self-assembled from 0.5 g/L aqueous solution of POSS-PBI-PEO.

Responsive behavior of POSS-PAI to F^- ion in THF

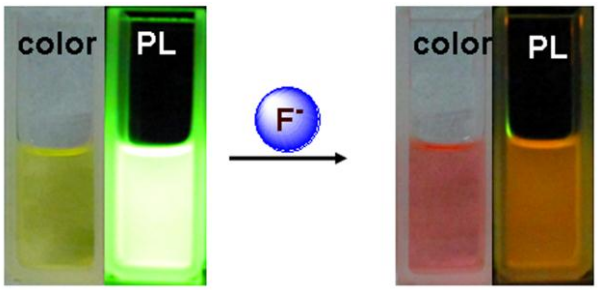

Figure S8. The distinct optical responses of POSS-PAI upon addition of 10 equiv of F^- in THF: [POSS-PAI] = 20 μM.

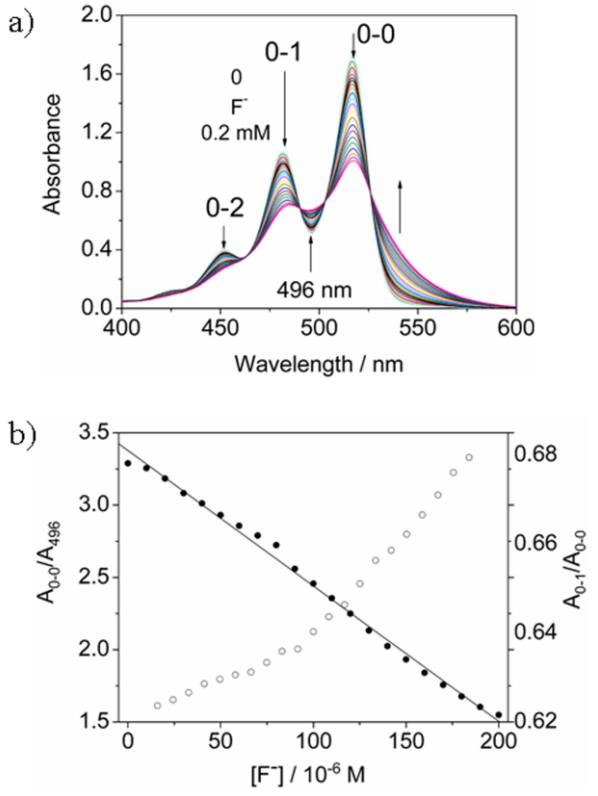

Figure S9. a) Absorbance spectra of POSS-PAI in THF (20 μM) with different F^- ion concentrations. b) Ratiometric calibration curves $A_{0\text{-}0}/A_{496}$ and $A_{0\text{-}1}/A_{0\text{-}0}$ as a function of F^- ion concentrations.

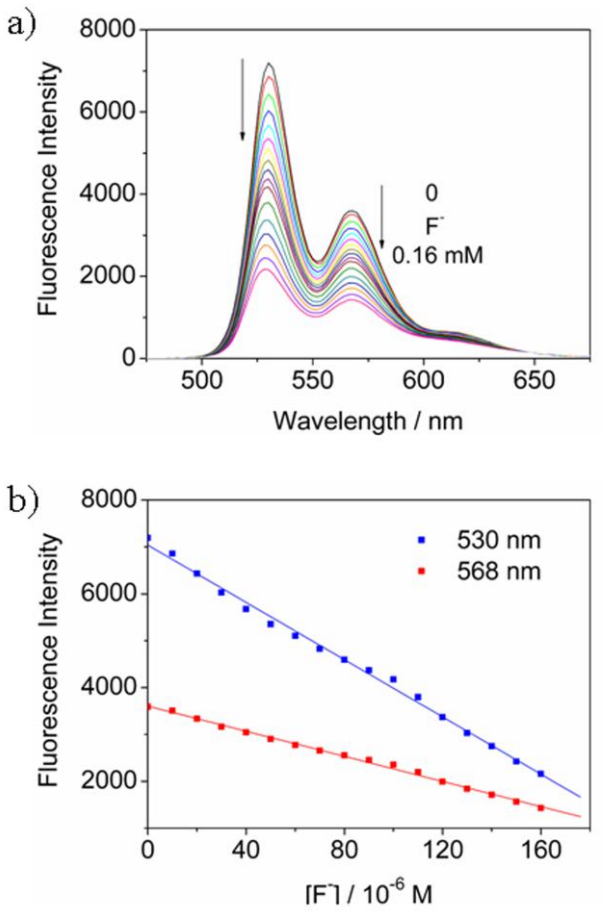

Figure S10. a) Fluorescence spectra (λ_{ex} = 450 nm) of POSS-PAI in THF (20 μM) with different F^- ion concentrations. b) Fluorescence intensity at 530 nm and 568 nm as a function of F^- ion concentrations.

Mechanism

^1H and ^{19}F NMR measurements were performed to demonstrate the reaction between POSS cages and F^- ions (Figure S11). The ^1H NMR spectrum of POSS-PAI reveals a broad peak at 0.6 ppm corresponding to Si-CH_2 of POSS and two doublets at 8.70 and 8.63 ppm corresponding to PAI protons, indicating that POSS-PAI exists in monomeric form at a high concentration of 1.0×10^{-3} M in $CDCl_3$. After the reaction of POSS-PAI with 20 equiv of F^- ion, both the two signals mentioned above disappear. This suggests the disappearance of POSS groups and the the formation of π-π stacking between PAI units. The ^{19}F NMR spectrum of TBAF displays a strong singlet at -129 ppm corresponding to the F^- ion. The reaction of F^- ion with POSS-PAI caused an

new signal at -115 ppm, which indicates the formation of covalent F-Si bonds. These results confirm that the sensitive and selective reaction between POSS and F^- ion occurs.

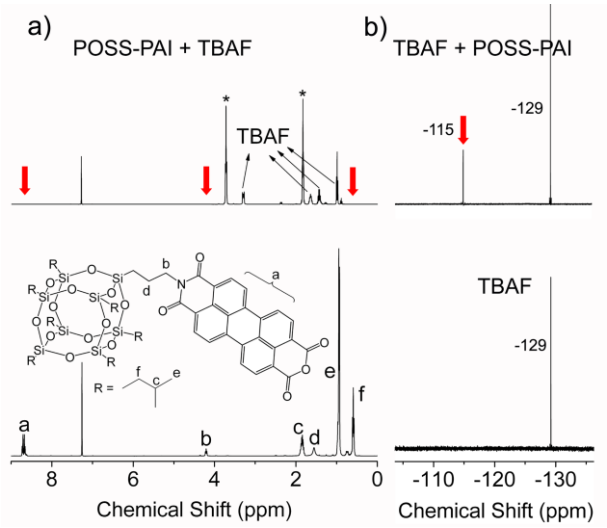

Figure S11. a) ^{1}H NMR (400 MHz) spectra of POSS-PAI (1.0×10^{-3} M) in $CDCl_3$ with addition of 20 equiv TBAF (1 M in THF). The two ^{1}H NMR peaks marked with * are ascribed to THF. b) ^{19}F NMR (400 MHz) spectra of TBAF (2.0×10^{-2} M) in $CDCl_3$ with addition of 1/20 equiv TBAF.

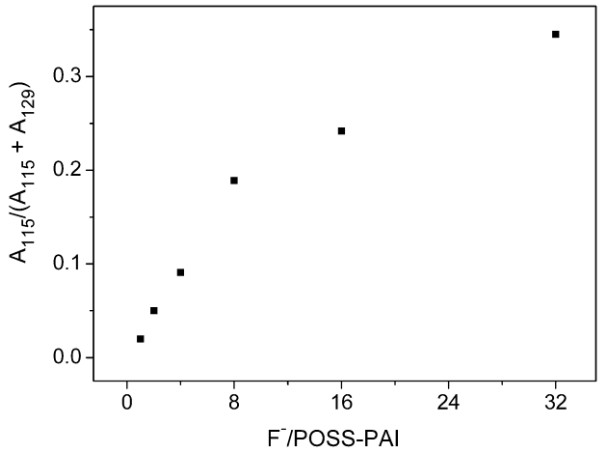

Figure S12. Titrations of POSS-PAI (1.0×10^{-3} M in $CDCl_3$) with TBAF recorded by ^{19}F NMR spectroscopy. A_{115} and A_{129} refer to the integral area of 115 and 129 ppm, respectively.

Influence of pH on the fluorescence of POSS-PBI-PEO NPs

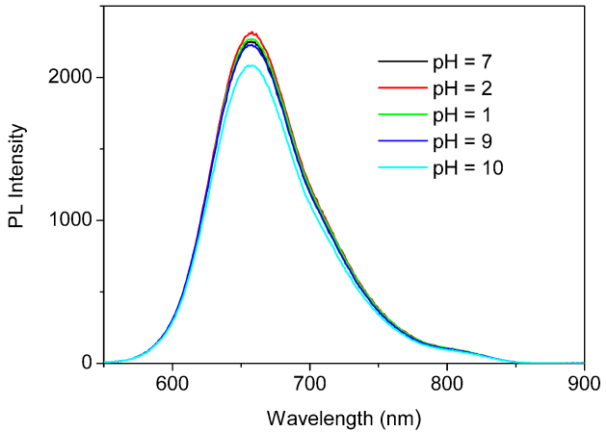

Figure S13. The influence of pH value of water on the fluorescence of POSS-PBI-PEO NPs.

Absorption spectra of POSS-PBI-PEO NPs upon the addition of F^-

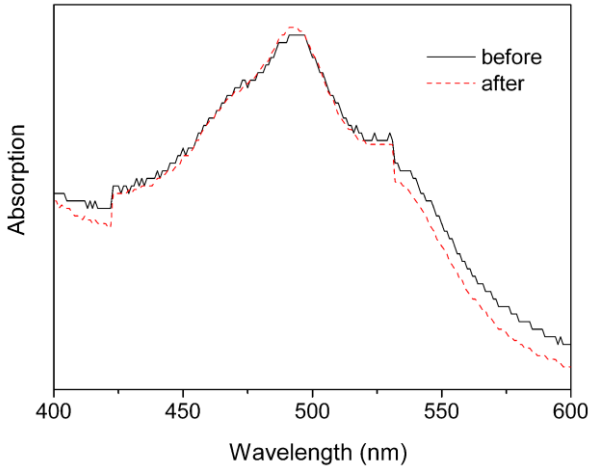

Figure S14. Absorption spectra of POSS-PBI-PEO NPs (5 μM) before and after the addition of F^- (1 mM) in aqueous solution.

Excitation spectrum of POSS-PBI-PEO NPs

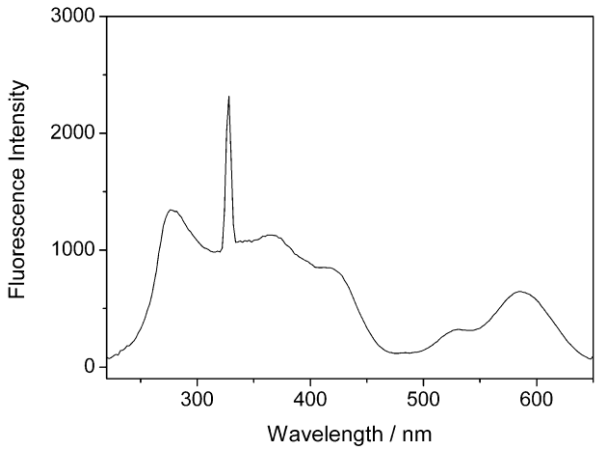

Figure S15. Excitation spectrum of POSS-PBI-PEO NPs (30 μM) in aqueous solution ($\lambda_{em.}$ = 660 nm).